Observation of the Kondo Effect in a Spin-$\frac{3}{2}$ Hole Quantum Dot

O. Klochan,[1,*] A. P. Micolich,[1] A. R. Hamilton,[1,†] K. Trunov,[2] D. Reuter,[2] and A. D. Wieck[2]

[1]*School of Physics, University of New South Wales, Sydney NSW 2052, Australia*

[2]*Angewandte Festkörperphysik, Ruhr-Universität Bochum, D-44780 Bochum, Germany*

(Received 24 February 2011; published 12 August 2011)

We report the observation of Kondo physics in a spin-$\frac{3}{2}$ hole quantum dot. The dot is formed close to pinch-off in a hole quantum wire defined in an undoped AlGaAs/GaAs heterostructure. We clearly observe two distinctive hallmarks of quantum dot Kondo physics. First, the Zeeman spin splitting of the zero-bias peak in the differential conductance is independent of the gate voltage. Second, this splitting is twice as large as the splitting for the lowest one-dimensional subband. We show that the Zeeman splitting of the zero-bias peak is highly anisotropic and attribute this to the strong spin-orbit interaction for holes in GaAs.

DOI: 10.1103/PhysRevLett.107.076805 PACS numbers: 73.63.Rt, 73.23.Ad, 73.61.Ey, 73.63.Kv

The observation of an unexpected minimum in the low temperature resistance of metals by de Haas in 1933 was ultimately explained 30 years later by Kondo as being due to interactions between a single magnetic impurity and the sea of conduction electrons in a metal [1,2]. More recently, there has been a resurgence of interest in the Kondo effect, following the discovery that the conductance of a few electron quantum dot in the Coulomb blockade regime is enhanced when the dot contains an odd number of electrons [3–5]. There is a direct analogy with the Kondo effect in metals, with the localized electron in the quantum dot acting as a magnetic impurity that interacts with the two-dimensional sea of electrons in the source and drain reservoirs.

Studies of the Kondo effect in bulk systems have progressed since the 1960s, with the focus shifting towards manifestations of Kondo physics in the strongly correlated electron systems formed in cuprates and heavy-fermion metals [6]. More precise control via improved electrostatic gate design has similarly allowed progress towards the study of more exotic manifestations of Kondo phenomena in quantum dots such as the integer-spin [7–9], two-impurity [10], and orbital Kondo effects [11]. Thus far, all quantum dot Kondo studies have involved electrons, and GaAs hole quantum dots present an interesting next step. Holes in GaAs originate from p-like orbitals and behave as spin-$\frac{3}{2}$ particles due to strong spin-orbit coupling [12]. In two- and one-dimensional systems, the spin-$\frac{3}{2}$ nature of holes leads to remarkable, highly anisotropic phenomena [13–17] not observed in electron systems, and new physics is expected for hole quantum dots also [18]. Studies of Kondo physics in hole quantum dots may also provide useful connections to recent studies in bulk strongly correlated systems [19,20].

Here we report the observation of the Kondo effect in a GaAs hole quantum dot. Because of the poor stability of conventional gate-defined modulation-doped structures [21], it has not been possible to define hole quantum dots small enough for studies of Kondo physics [4]. Instead, we follow the approach of Sfigakis *et al.* [22], where roughness in the walls of a wet-etched quantum wire led to the formation of an incidental quantum dot exhibiting Kondo physics as the wire approached pinch-off. A key advantage to this approach is the ability to obtain an independent estimate of the effective Landé g factor g^*. Using this we have fabricated a small hole quantum dot and conclusively demonstrate the ''smoking gun'' for Kondo physics [23]—a splitting of the zero-bias peak in the differential conductance that opens as $2g^*\mu_B B$ in response to an in-plane magnetic field B and is independent of the gate voltage [4,5]. In contrast to electrons, we find that the field splitting of the zero-bias peak is highly anisotropic.

We used a heterostructure consisting of the following layers grown on a (100)-oriented substrate: 1 μm undoped GaAs, 160 nm undoped AlGaAs barrier, 10 nm undoped GaAs spacer, and a 20 nm GaAs cap degenerately doped with carbon for use as a metallic gate [24,25]. A (100) heterostructure was used to avoid the crystallographic asymmetries that plague (311)A heterostructures [16,17]. Ohmic contacts are made with AuBe alloy annealed at 490 °C for 60 s. Our devices are remarkably stable, owing to population with holes electrostatically rather than by ionized modulation dopants [24,25]. A 300 nm long by 300 nm wide quantum wire aligned along the $[01\bar{1}]$ crystallographic direction is fabricated by electron beam lithography, as shown in the lower left inset in Fig. 1(a). The quantum wire is defined by shallow etching the doped cap to a depth of $\sim$25 nm to form three gates—a central top gate negatively biased to V_{TG} to control the hole density and two side gates positively biased to V_{SG} to control the electrostatic width of the wire [17,25]. The quantum dot forms as the wire approaches pinch-off, as discussed in the following paragraph. All data were obtained at $V_{\mathrm{TG}} = -0.67$ V corresponding to a 2D hole density $p = 2 \times 10^{11}$ cm^{-2} and mobility $\mu = 450\,000$ cm^2/Vs. We used standard lock-in techniques to measure the

two-terminal differential conductance $G'(V_{SD})$ with a variable dc source-drain bias V_{SD} added to a constant 15 μV ac excitation at 5 Hz. A constant series resistance of 30.5 kΩ was subtracted from all measurements presented. The experiment was performed in a dilution refrigerator with a base temperature of 25 mK, which featured an *in situ* rotator that enabled the sample to be reoriented with respect to the applied magnetic field B without the sample temperature exceeding 200 mK [26].

Figure 1(a) shows the linear conductance $G = G'(V_{SD} = 0)$ versus V_{SG} with the six quantized conductance plateaus confirming ballistic transport through the device. The quantum dot forms at $G < 2e^2/h$ due to a combination of microscopic deviations in confining potential due to etch roughness in the gates [22] and self-consistent electrostatic effects [27]. The presence of a bound state in this system is revealed by the evolution of G versus V_{SG} with an increasing in-plane magnetic field aligned parallel $B_\parallel$ [Fig. 1(c)] and perpendicular $B_\perp$ [Fig. 1(d)] to the wire at $G < 2e^2/h$. In both cases, plateaus at e^2/h and $3e^2/h$ emerge, indicating the onset of spin splitting [28], accompanied by sharp resonances signalling formation of a bound state within the wire [22,29–31]. We will show later in Fig. 2(a) that this bound state is not an impurity effect, as it is robust to gate-induced lateral shifting of the 1D channel [32]. Coupling of the magnetic field to orbital motion [33] may be responsible for the differences in resonant structure between Figs. 1(c) and 1(d), as any random disorder potential should be constant given that both orientations were measured during a single cooldown.

A study of the zero-bias peak (ZBP) in the differential conductance provides additional evidence for quantum dot formation. Figure 1(b) shows G' versus V_{SD} at a range of V_{SG} spanning $0 < G < 1.2 \times 2e^2/h$, with two traces highlighted. Under a single particle picture, G' should depend quadratically on V_{SD} with a minimum at $V_{SD} = 0$ [34], as observed for the blue trace at $G > 2e^2/h$ in Fig. 1(b). In contrast at $G < 2e^2/h$, G' shows a pronounced peak at $V_{SD} = 0$ superimposed upon a parabolic background [red trace, Fig. 1(b)], known as the zero-bias peak. We observe the ZBP at conductances as low as $10^{-3} \times 2e^2/h$, consistent with previous work [22,35,36]. This is demonstrated in the upper right inset in Fig. 1(a) and in Fig. 1 of Ref. [37], where we replot the data in Fig. 1(b) on a logarithmic conductance scale.

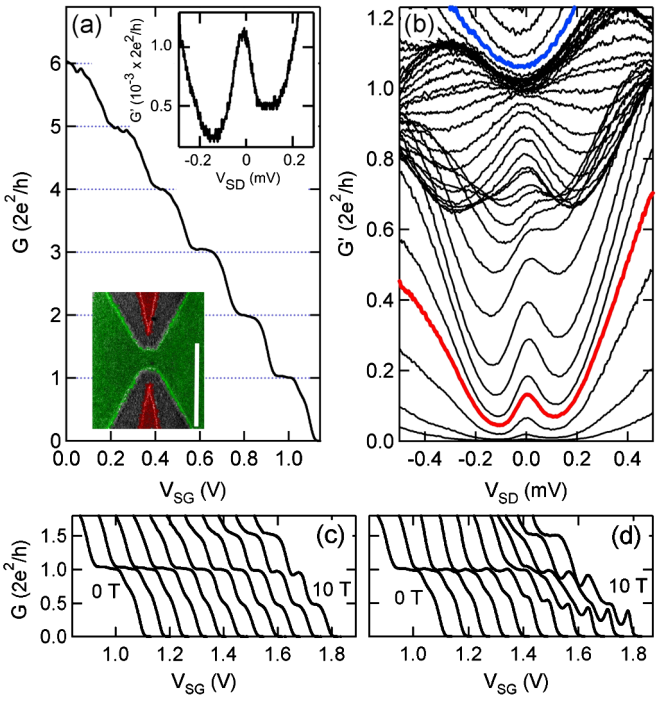

FIG. 1 (color online). (a) Linear conductance G versus side-gate voltage V_{SG} for our device; the dot forms at $G < 2e^2/h$ (see the text). Lower left inset: Scanning electron micrograph of the device with the top gate (green) and side gates (red) separated by etched trenches (gray). The scale bar indicates 1 μm. Upper right inset: Differential conductance G' versus dc source-drain bias V_{SD} at a side-gate voltage $V_{SG} = 1.115$ V showing the zero-bias peak at $10^{-3} \times 2e^2/h$. (b) G' versus V_{SD} for various V_{SG} starting at 1.1 V (bottom) and stepping sequentially by -5 mV to 0.9 V (top). The red trace ($V_{SG} = 1.085$ V, $G < e^2/h$) shows enhanced conductance centered at $V_{SD} = 0$, while the blue trace ($V_{SG} = 0.91$ V, $G > 2e^2/h$) shows the standard parabolic dependence of G' on V_{SD}. (c),(d) G versus V_{SG} for increasing in-plane magnetic field (c) parallel to ($B_\parallel$) and (d) perpendicular to ($B_\perp$) the wire. Traces were obtained with an increment of +1 T and offset to the right by +0.07 V for clarity.

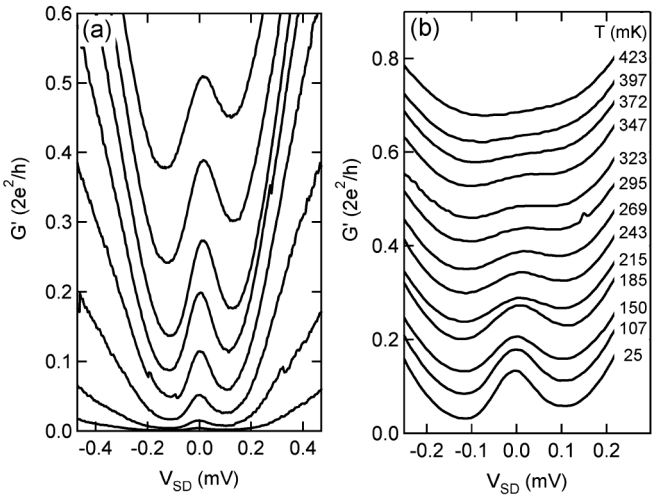

FIG. 2. (a) Asymmetric bias study of G' versus V_{SD} at various V_{SG}. Each trace directly corresponds to one in Fig. 1(b), with the two side-gate voltages set such that they differ by 0.5 V but their average equals the V_{SG} in Fig. 1(b). The lowest trace has $V_{SG}^1 = 0.85$ V and $V_{SG}^2 = 1.35$ V, which average to 1.1 V to match V_{SG} for the lowest trace in Fig. 1(b). Moving upwards, both side gates are sequentially incremented by -5 mV for each trace; the uppermost trace has an average $V_{SG} = 1.065$ V. (b) G' versus V_{SD} at fixed $V_{SG} = 1.085$ V for different temperatures T. Traces are sequentially offset by $+0.05 \times 2e^2/h$ from the bottom.

To demonstrate that the ZBP is robust and not due to random disorder [38], we have studied the ZBP as the wire is shifted laterally. We do this by repeating each measurement in Fig. 1(b) with a voltage offset of 0.25 V added to side gate 1 and subtracted from side gate 2, such that the average bias is maintained to facilitate direct comparison. This results in a lateral shift of the wire by ≈ 60 nm [32] and gives the data shown in Fig. 2(a) For traces below e^2/h, there is almost no change in the ZBP compared to the data from the unshifted channel in Fig. 1(b), confirming that the ZBP is not disorder-induced. Equivalent data were obtained when we shifted the channel in the opposite direction (see Fig. 2 of Ref. [37]). To further check the consistency of our ZBP with the known Kondo physics of electron quantum dots, in Fig. 2(b) we show the evolution of the red trace from Fig. 1(b) with temperature T. The peak widens and decreases in amplitude with increasing T, consistent with previous studies [5].

We now focus on the magnetic field dependence of the zero-bias peak looking for (a) the g^* anisotropy characteristic of spin-$\frac{3}{2}$ holes and (b) the distinctive $2g^*\mu_B B$ peak splitting of Kondo physics. We begin by examining the evolution of the ZBP with $B_\parallel$ in Fig. 3(a). Initially, no splitting is resolved and the only change is a widening of the zero-bias peak. However, at $B_\parallel \approx 4$ T two peaks become resolved, and these separate in V_{SD} as $B_\parallel$ is increased further. The behavior is very different with an in-plane field $B_\perp$ applied perpendicular to the wire [Fig. 3(b)]. Here the peak shows no splitting even at the highest field $B_\perp = 10$ T; instead, the peak is gradually reduced in amplitude and ultimately suppressed entirely. This anisotropic behavior matches the underlying g^* anisotropy of the 1D wire [17] in which the dot resides. We return to this anisotropy in the final discussion and now continue with quantitative analysis of the peak splitting with $B_\parallel$.

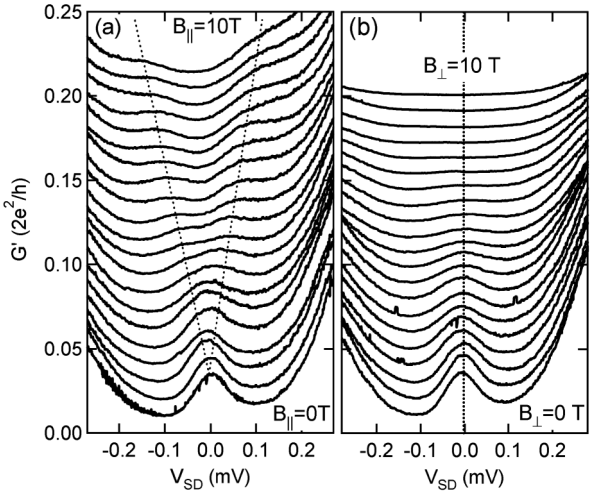

FIG. 3. G' versus V_{SD} at $V_{SG} = 1.105$ V measured for in-plane magnetic fields ranging from 0 to 10 T oriented (a) parallel to ($B_\parallel$) and (b) perpendicular to ($B_\perp$) the wire. Traces were obtained with a +0.5 T increment and sequential vertical offset of $+0.01 \times 2e^2/h$ from the bottom.

As pointed out by Cronenwett, Oosterkamp, and Kouwenhoven in Ref. [5], the most distinct sign of the quantum dot Kondo effect is a gate-voltage-independent ZBP split by $2g^*\mu_B B$. Figure 4(a) shows G' versus V_{SD} at various V_{SD} at $B_\parallel = 8$ T. The two vertical dotted lines in Fig. 4(a) pass through the field-split zero-bias peaks over more than 3 orders of magnitude in conductance, demonstrating the gate-voltage independence of the peak splitting. Turning to the splitting as a function of the field, in Fig. 4(b) we plot the peak location in V_{SD} for the traces in Fig. 3(a), where two peaks can be clearly resolved against $B_\parallel$. The peak locations are determined by eye, and the error bars are estimated knowing that the ZBP sits on a parabolic background with a slight linear asymmetry from the way that V_{SD} is applied in the measurement circuit. The ZBP clearly splits linearly with $B_\parallel$ in Fig. 4(b), giving $g^*_{ZBP} = 0.23 \pm 0.05$ if we assume a splitting $eV_{SD} = 2g^*_{ZBP}\mu_B B$. The data will justify this assumption below. We repeated this analysis at eight different conductances between 10^{-3} and $0.5 \times 2e^2/h$ giving the solid circles plotted in Fig. 4(c). The error bars are obtained from a regression analysis of linear fits such as that in Fig. 4(b). The g^*_{ZBP} values obtained are constant over 3 orders of magnitude in G, in agreement with Fig. 4(a), and give an average $g^*_{ZBP} = 0.236 \pm 0.012$.

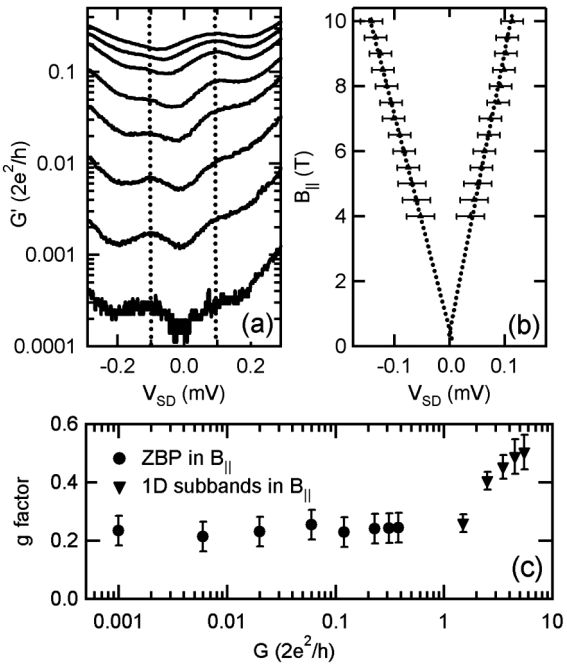

FIG. 4. (a) Plot of G' versus V_{SD} at various V_{SG} at fixed $B_\parallel = 8$ T demonstrating the gate-voltage independence of the splitting. (b) Location of the spin-split zero-bias peaks in V_{SD} (x axis) versus $B_\parallel$ for the data from Fig. 3(a). (c) Measured g factor g^* for $B_\parallel$ versus G for the zero-bias peak (solid circles) at $G < 2e^2/h$ and 1D subbands (solid triangles) at $G > 2e^2/h$.

A natural question is, how do we know that the peak splitting is given by $2g^*\mu_B B$ rather than $g^*\mu_B B$, which would increase the g^* extracted from the data by a factor of 2? The key advantage of our device is that we can use 1D subband spectroscopy [28] to independently measure g^* in the limit where G approaches $2e^2/h$ from above. This allows us to corroborate our measurement of g^*_{ZBP}. We measure g^*_{1D} for the first five 1D subbands by using the method in Ref. [17] and the usual Zeeman expression $g^*_{\mathrm{1D}}\mu_B B$ for 1D subbands [28]. The corresponding transconductance gray scale is in Fig. 3 of Ref. [37]. The resulting g^*_{1D} values, plotted as solid triangles in Fig. 4(c), decrease linearly as G approaches $2e^2/h$. This linear decrease is distinctive of holes in (100) heterostructures [17]. However, the most significant aspect is that the $g^*_{\mathrm{1D}} = 0.25 \pm 0.03$ obtained for the lowest 1D subband by assuming the 1D splitting goes as $g^*\mu_B B$ is in excellent agreement with g^*_{ZBP} obtained by assuming the ZBP splitting goes as $2g^*\mu_B B$. This is smoking gun evidence confirming our observation of Kondo physics in a hole quantum dot [4,5,23].

We conclude by discussing some key implications of our findings. The magnitude and anisotropy of g^*_{ZBP} closely match those of g^*_{1D} for the lowest 1D subband. This suggests that g^*_{ZBP} is set by the prevailing g^* of the environment hosting the dot. It agrees with quantum dots [5], where the splitting of the ZBP gives the same g^* as bulk GaAs, and with carbon nanotubes [39]. The fact that a spin-$\frac{3}{2}$ system produces no radical change in the observed Kondo physics is interesting, as it implies that the process relies only on the presence of a doubly degenerate quantum dot level to mediate transport between the reservoirs and not its precise nature or spin. This is in accordance with recent studies of more exotic manifestations of Kondo physics in quantum dots [7–11]. However, a spin-$\frac{3}{2}$ system may ultimately present more subtle changes; for example, confinement-induced mixing [40] between heavy-hole and light-hole subbands (i.e., states with total angular momentum quantum numbers $m_j = \pm\frac{3}{2}$ and $\pm\frac{1}{2}$, respectively) may alter the relevant scales in the problem. Further studies in this direction would be useful, including both theoretical work and measurements from improved device geometries. Finally, we comment briefly on the bearing of our results on studies of the 0.7 anomaly [41] in 1D systems. Although we observe a plateaulike feature near $0.7 \times 2e^2/h$ in our device [see Figs. 1(a), 1(c), and 1(d)], the presence of the resonant structure in the linear conductance precludes any direct and definitive link between the 0.7 anomaly and the behavior we observe for our zero-bias peak. We emphasize that the gate-voltage-independent Zeeman splitting of our ZBP points conclusively to the quantum dot Kondo effect, in contrast with the gate-voltage-dependent zero-bias anomaly splitting observed in undoped quantum wires by Sarkozy *et al.* [35]. The characteristics of our zero-bias peak are very different from those of the zero-bias anomaly in quantum wires. The two effects clearly have a different origin, which agrees with the suggestion by Sarkozy *et al.* [35] that the zero-bias anomaly is a fundamental property of quantum wires and suggests that it may involve processes beyond Kondo physics alone.

This work was funded by the Australian Research Council (Grants No. DP0772946, No. DP0986730, and No. FT0990285). We thank U. Zülicke for helpful discussions, L. A. Yeoh and A. Srinivasan for development of the low temperature rotator, and J. Cochrane for technical support.

*klochan@phys.unsw.edu.au
†Alex.Hamilton@unsw.edu.au

[1] W. J. de Haas, J. de Boer, and G. J. van den Berg, Physica (Utrecht) **1**, 1115 (1934).
[2] J. Kondo, Prog. Theor. Phys. **32**, 37 (1964).
[3] L. P. Kouwenhoven and L. I. Glazman, Phys. World **14**, 33 (2001).
[4] D. Goldhaber-Gordon *et al.*, Nature (London) **391**, 156 (1998).
[5] S. M. Cronenwett, T. H. Oosterkamp, and L. P. Kouwenhoven, Science **281**, 540 (1998).
[6] G. R. Stewart, Rev. Mod. Phys. **73**, 797 (2001).
[7] S. Sasaki *et al.*, Nature (London) **405**, 764 (2000).
[8] W. G. van der Wiel *et al.*, Phys. Rev. Lett. **88**, 126803 (2002).
[9] G. Granger *et al.*, Phys. Rev. B **72**, 165309 (2005).
[10] H. Jeong, A. M. Chang, and M. R. Melloch, Science **293**, 2221 (2001).
[11] P. Jarillo-Herrero *et al.*, Nature (London) **434**, 484 (2005).
[12] R. Winkler *et al.*, Phys. Rev. Lett. **85**, 4574 (2000).
[13] S. J. Papadakis *et al.*, Phys. Rev. Lett. **84**, 5592 (2000).
[14] R. Danneau *et al.*, Phys. Rev. Lett. **97**, 026403 (2006).
[15] L. P. Rokhinson, L. N. Pfeiffer, and K. W. West, Phys. Rev. Lett. **96**, 156602 (2006).
[16] O. Klochan *et al.*, New J. Phys. **11**, 043018 (2009).
[17] J. C. H. Chen *et al.*, New J. Phys. **12**, 033043 (2010).
[18] T. Andlauer and P. Vogl, Phys. Rev. B **79**, 045307 (2009).
[19] K. Suzuki *et al.*, Phys. Rev. B **82**, 054519 (2010).
[20] A. Ślebarski *et al.*, Phys. Rev. B **82**, 235106 (2010).
[21] K. Ensslin, Nature Phys. **2**, 587 (2006).
[22] F. Sfigakis *et al.*, Phys. Rev. Lett. **100**, 026807 (2008).
[23] Y. Meir, N. S. Wingreen, and P. A. Lee, Phys. Rev. Lett. **70**, 2601 (1993).
[24] W. R. Clarke *et al.*, J. Appl. Phys. **99**, 023707 (2006).
[25] O. Klochan *et al.*, Appl. Phys. Lett. **89**, 092105 (2006).
[26] L. A. Yeoh *et al.*, Rev. Sci. Instrum. **81**, 113905 (2010).
[27] Y. Yoon *et al.*, Phys. Rev. Lett. **99**, 136805 (2007).
[28] N. K. Patel *et al.*, Phys. Rev. B **44**, 13 549 (1991).
[29] P. L. McEuen *et al.*, Surf. Sci. **229**, 312 (1990).
[30] C.-T. Liang *et al.*, Phys. Rev. Lett. **81**, 3507 (1998).
[31] Y. Komijani *et al.*, Europhys. Lett. **91**, 67 010 (2010).
[32] L. I. Glazman and I. A. Larkin, Semicond. Sci. Technol. **6**, 32 (1991).
[33] C. H. L. Quay *et al.*, Nature Phys. **6**, 336 (2010).
[34] L. Martín-Moreno *et al.*, J. Phys. Condens. Matter **4**, 1323 (1992).

[35] S. Sarkozy *et al.*, Phys. Rev. B **79**, 161307 (2009).
[36] Y. Ren *et al.*, Phys. Rev. B **82**, 045313 (2010).
[37] See Supplemental Material at http://link.aps.org/supplemental/10.1103/PhysRevLett.107.076805 for supplementary figures.
[38] T.-M. Chen *et al.*, Phys. Rev. B **79**, 153303 (2009).
[39] J. Nygård *et al.*, Nature (London) **408**, 342 (2000).
[40] U. Zülicke, Phys. Status Solidi C **3**, 4354 (2006).
[41] K. J. Thomas *et al.*, Phys. Rev. Lett. **77**, 135 (1996).